Scientific paper

The Effect of Temperature and Fe^{3+} Concentration on the Formation of γ-Fe_2O_3 Nanoparticles Embedded in Silica Matrix

Oana Ştefănescu,[1,*] Corneliu Davidescu[1] and Paul Barvinschi[2]

[1] *Faculty of Industrial Chemistry and Environmental Engineering, University „Politehnica", P-ta Victoriei no.2, 30006, Timisoara, Romania*

[2] *Faculty of Physics, West University, Bv. V. Parvan no. 4, 300223 Timisoara, Romania*

* *Corresponding author: E-mail: oana.stefanescu@chim.upt.ro*

Received: 13-11-2009

Abstract

The paper presents a study on the formation and thermal stability of γ-Fe_2O_3 nanoparticles within the silica matrix depending on the Fe(III) carboxylate-type precursors, their annealing temperature and the concentration of Fe^{3+}. Obtaining of the precursors, within the pores of the gel, bases on the redox reaction between $Fe(NO_3)_3$ and diols: ethylene glycol (EG) and 1,4 buthane diol (1,4 BG), respectively. Thus, we have prepared gels with different Fe_2O_3/SiO_2 ratios (20, 30, 50, 70 wt% Fe_2O_3) which were annealed in the temperature range **573-1273 K**.

The formation and stability of the single γ-Fe_2O_3 phase within the pores is strongly influenced by the reducing atmosphere generated upon thermal decomposition of the Fe(III) carboxylates. The XRD analysis evidenced a much stronger crystallization of γ-Fe_2O_3 in case of the nanocomposites synthesized with 1,4 BG than with EG.

The magnetic measurements confirm the crystallinity of γ-Fe_2O_3 within the silica matrix.

Keywords: Carboxylates, γ-Fe_2O_3, silica matrix, thermal analysis, XRD

1. Introduction

In the last years, the iron oxide-silica nanocomposites have been the subject of intense research due to their potential applications in magnetic-tape media,[1] magneto-optical devices,[2] magnetic refrigerators,[3] bioprocessing,[4] catalysis and ferrofluids.[5,6] The silica aerogels display most of the conditions required by the host matrix: chemical inertness, large surface areas, high porosity, pores in the nanometer range and high transparency.[7] The use of an inorganic host matrix for nanocrystalline particles could be an effective way for the limitation of particles size distribution and control on the homogenous dispersion of ultrafine metal oxides particles. Magnetic iron oxide nanoparticles exhibit enhanced surface effects, superparamagnetic behavior and changes in saturation magnetisation and coercive fields.[8]

Maghemite (γ-Fe_2O_3) nanoparticles present unique magnetic, catalytic and optical properties compared to the bulk material.[9] Embedding of magnetic particles within the silica matrix prevents their aggregation at temperatures up to 1273K and facilitates the stabilization of γ-Fe_2O_3.[10] The sol-gel method is a promising way for obtaining of iron oxide nanoparticles within an ordered silica matrix. Silica and iron oxide precursors are mixed in solution and condensed by the sol-gel process in order to obtain a mixed metallic oxides network.

In previous papers, we have elaborated the synthesis method for some carboxylate-type complex combinations based on the redox reaction between transitional metal nitrates and diols.[11,12] Regarding the Fe_2O_3 system obtained from the Fe(III) carboxylate type complexes, we have pursued the formation of the single γ-Fe_2O_3 phase embedded in a SiO_2 matrix.[13,14]

The Fe(III) carboxylate-type complex combinations (glyoxylate $[Fe_2(C_2H_2O_4)_2(OH)_2(H_2O)_2]$ and succinate $[Fe_2(C_4H_4O_4)(OH)_4(H_2O)_2] \cdot 1.5\ H_2O$), embedded in the pores of silica gels, generate a reducing atmosphere (CO/C) by thermal decomposition. The reducing atmosp-

here achieves the in-situ redox equilibria $Fe^{3+} \rightarrow Fe^{2+}$ and $2\ Fe^{2+} + 3/2\ O_2 \rightarrow Fe_2O_3$, respectively, responsible for the formation of the crystalline γ-Fe_2O_3 phase. The composition of the reducing atmosphere depends on the nature of respective diols and influences the degree of crystallinity of the oxide γ-Fe_2O_3 phase.

In this paper we present a study on the formation of the γ-Fe_2O_3 nanocrystallites as the single phase within the SiO_2 matrix using an original synthesis method (sol-gel), which allows the stabilisation of γ-Fe_2O_3 at high temperatures. The formation of γ-Fe_2O_3 depends on the Fe(III) carboxylate-type combination embedded in the pores of the silica gel (glyoxylate, succinate), the thermal treatment temperature **(573–1273 K)** and the mass ratio Fe_2O_3/SiO_2 (20, 30, 50, 70 wt%).

2. Experimental

The gel samples were synthesized by the modified sol-gel method,[15] from a mixture of $Fe(NO_3)_3 \cdot 9H_2O$, ethylene glycol (EG) and 1,4 buthane diol (1,4 BG), respectively, tetra-ethyl orthosilicate (TEOS), ethanol as solvent and concentrated nitric acid (HNO_3). All reagents were of high purity (>98%), product of Merck.

The ethanolic TEOS solution was added drop wise, under magnetic stirring, to the mixture $Fe(NO_3)_3 \cdot 9H_2O$-diol (EG or 1,4 BG), for the ratios Fe_2O_3/SiO_2: 20, 30, 50, 70 wt%. **The molar ratio NO^-_3: diol used in the synthesis was: NO^-_3: EG = 1:0.75 and NO^-_3: 1,4 BG = 1: 0.56, representing 50% diol excess, related to the stoichiometry.** The samples were denoted as follows: E_x for gels synthesized with EG and B_x for gels synthesized with 1,4 BG, where x = 20, 30, 50, 70 wt%. The obtained gels were dried at 313 K, 1h, and subsequently heated at 403K, 3 h, when the redox reaction between NO_3^- and diol took place with the formation of the Fe(III) carboxylate-type complex combination within the pores of the silica gel. The obtained powders were characterized by thermal analysis and FT-IR spectrometry.

The gels (E_x and B_x) obtained at 403 K, were annealed in the temperature range **573–1273 K**, in air, for 3 h, in a Nabertherm furnace, in order to obtain the oxides. The crystalline phases obtained in the composites were identified by X-ray diffraction on a D8 Advanced- Bruker AXS diffractometer, using Mo- Kα radiation (λ_{Mo} = 0.7093 Å). **The transmission electron microscopy was performed with a JEOL JEM 1010 microscope.**

For monitoring the evolution of the redox reaction between Fe(III) nitrate and diols, the gels were characterized by thermal analysis using a 1500 D MOM Budapesta derivatograph. The thermal behaviour of the complex combinations embedded in the gels was followed by a Diamond Perkin Elmer thermo-balance in air, up to 773 K, with a heating rate of 10 K/min, with the sample mass of ~30 mg.

The samples were characterized by FT-IR spectrometry on a Shimadzu Prestige-21 a FT-IR spectrometer, in KBr pellets, in the range 400–4000 cm^{-1}. Magnetic measurements were performed by a laboratory installation with the data acquisition system.

3. Results and Discussion

The formation of the Fe(III) carboxylate-type complex combinations within the pores of the gel was analyzed by thermal analysis and FT-IR spectrometry. Figure 1 presents the TG and DTA curves of the gel B_{30} heated at 313 K. The DTA curve presents an exothermic effect at 343 K attributed to the redox reaction between $Fe(NO_3)_3$ and 1,4 BG with the formation of the Fe(III) complex combination (succinate) within the pores. The second

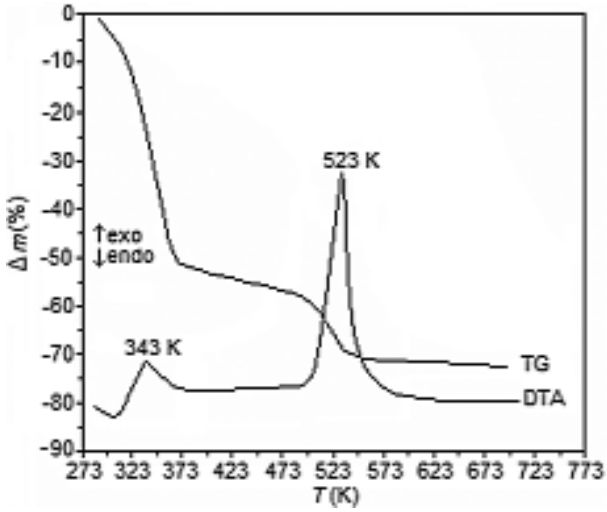

Figure 1. TG and DTA curves of the gel B_{30} heated at 313K

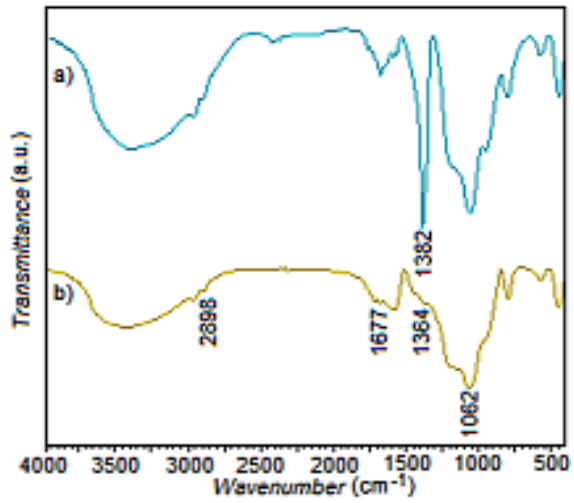

Figure 2. FT-IR spectra of the gel B_{30} heated at 313 K (a) and 403 K (b)

exotherm at 523 K corresponds to the oxidative decomposition of the formed complex combination. The mass losses on the TG, in the first stage, correspond to the elimination of volatile products: H_2O, NO_x, and in the second stage, to the elimination of the oxidation products CO, CO_2 and condensation products of the matrix.

As a result of thermal analysis data, we have established 403 K as the optimal synthesis temperature for the complex combinations within the pores.

Figure 2 presents the FT-IR spectra of the gel B_{30} at 313 K (spectrum a) which evidences a clear band at 1382 cm^{-1} attributed to NO_3^-, free in the pores of the gel. The spectrum (b) corresponding to the gel thermally treated at 403 K shows the disappearance of the band at 1382 cm^{-1} and the appearance of the bands characteristic for the complex combination in the pores: $\nu_{as}(COO^-)$ at 1677 cm^{-1} and $\nu_s(COO^-)$ at1364 cm^{-1}.[16] In the range 2800–3000 cm^{-1} (spectra a and b) the bands characteristic for the groups $–CH_2–$, $–CH_3$ from the carboxylates as well as for the diols chemically bonded within the matrix are registered.[17] The intense band at 1062 cm^{-1} is attributed to the asymmetric stretching vibration ν_{as}(Si-O-Si).[18]

All synthesized samples (E_x, B_x) present similar thermal and FT-IR behavior.

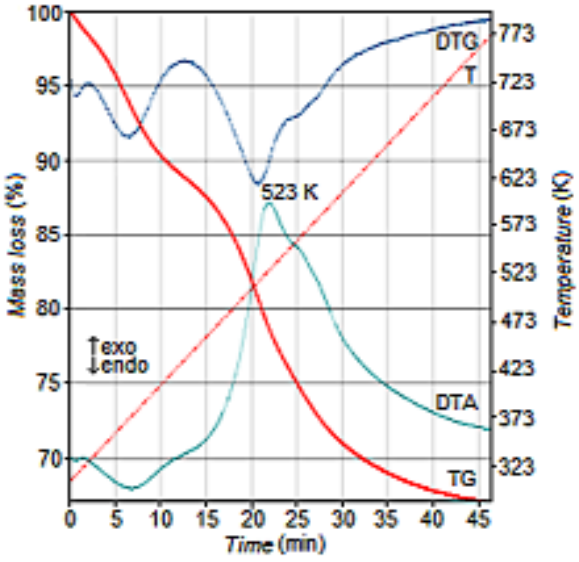

Figure 3. Thermal analysis curves of the gel B_{20} thermally treated at 403 K

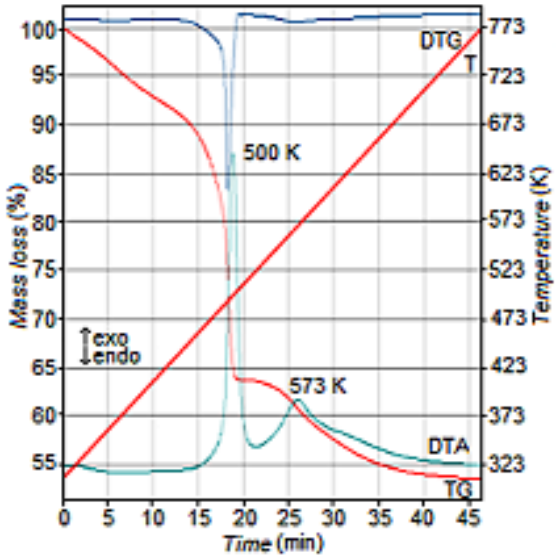

Figure 5. Thermal analysis curves of the gel B_{50} thermally treated at 403 K

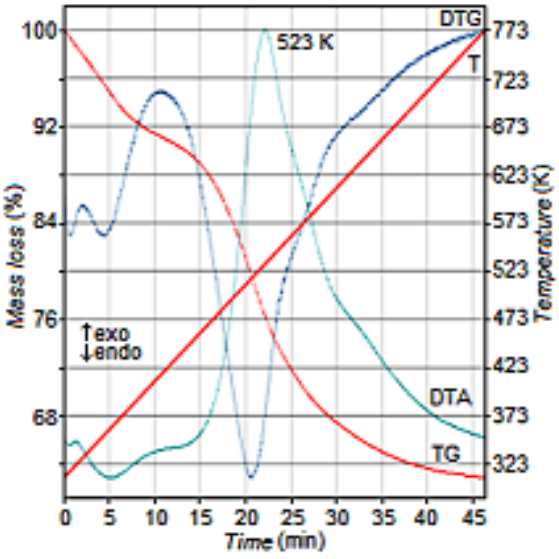

Figure 4. Thermal analysis curves of the gel B_{30} thermally treated at 403 K

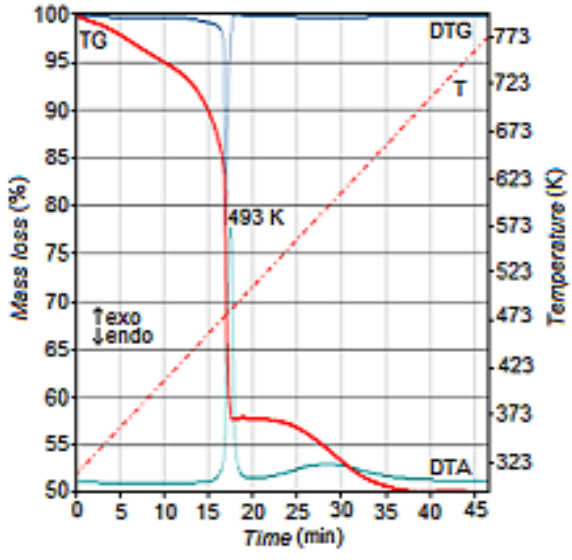

Figure 6. Thermal analysis curves of the gel B_{70} thermally treated at 403 K

Figures 3–6 present the thermal analysis curves for the gels B_x synthesized with 1,4 BG. The registered thermal processes justify the formation of the complex combination within the pores of the gels, in all cases. The evolution of the thermal analysis curves is influenced by the composition of the gels.

At low concentrations of 20 and 30 wt% Fe_2O_3/SiO_2, the Fe(III) complex combination is found in a lower quantity, uniformly distributed within the pores of the gels. The thermal decomposition process (Figures 3 and 4) with the elimination of CO, accompanied by a large exothermic effect at ~523 K proceeds with a low rate. The mass loss up to 773 K is attributed to the elimination of the poly-condensation products of the silica matrix.

At higher concentrations of 50 and 70 wt% Fe_2O_3/SiO_2, the decomposition of the complex combination (Figures 5 and 6) takes place at a higher rate in a narrower temperature range with a pronounced exothermic effect at ~500 K. The mass loss in this range mostly corresponds to the oxidative decomposition of the complex combination. The weak exothermic effect at ~573 K, with a mass loss, is attributed to the burning of the organic chain of the diol, bonded within the silica matrix during the poly-condensation process.[17]

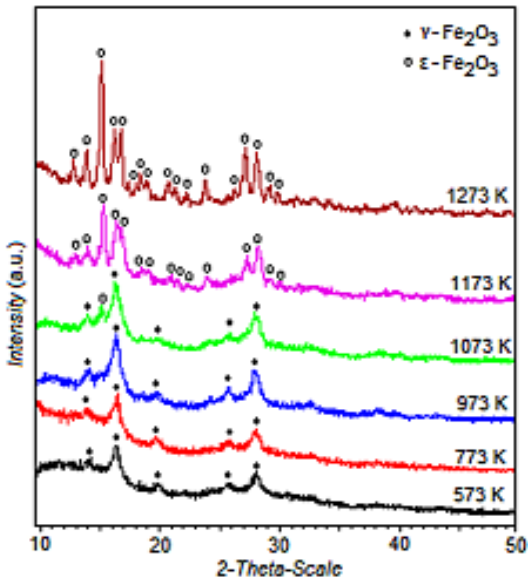

Figure 7. XRD patterns of the gel B_{50} annealed at different temperatures

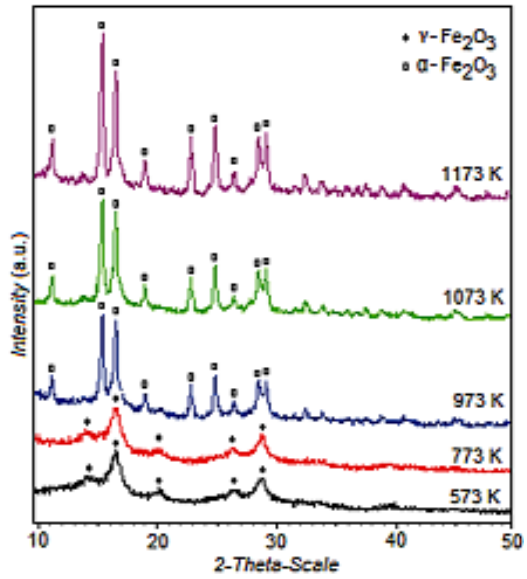

Figure 9. XRD patterns of the gel B_{70} annealed at different temperatures

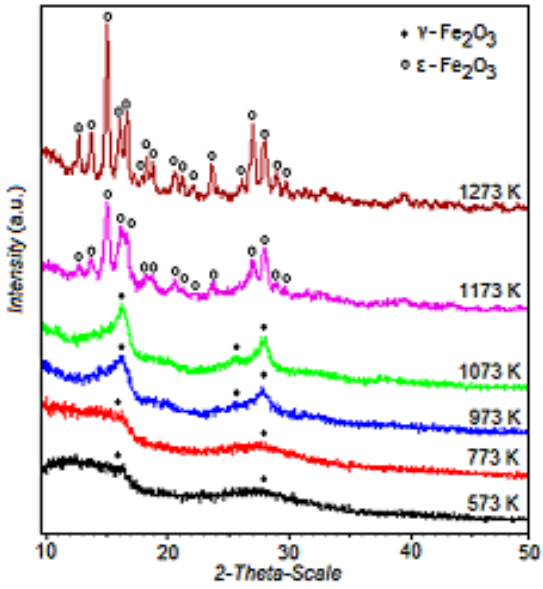

Figure 8. XRD patterns of the gel E_{50} annealed at different temperatures

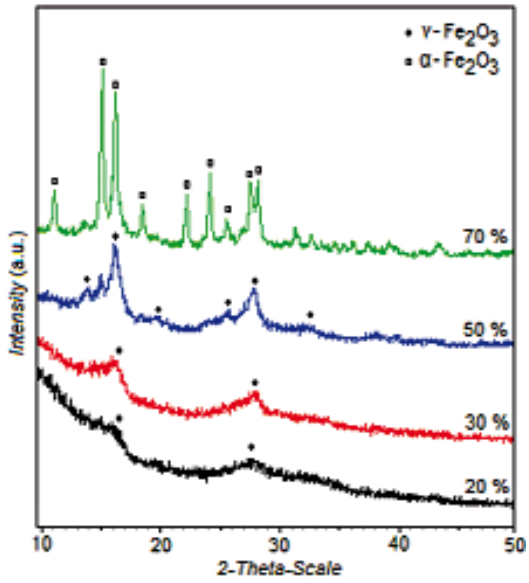

Figure 10. XRD patterns of gels B_x annealed at 1073 K

For all gels (B_x, E_x), the thermal decomposition process of the Fe(III) carboxylate type complex combination takes place within the pores of the gels with the generation of a reducing atmosphere (CO/C). The composition of the reducing atmosphere depends on the synthesized complex combination (on the nature of the diol). The reducing atmosphere (CO + 3C) generated upon the thermal decomposition of the Fe(III) succinate-type complex combination ($[Fe_2(C_4H_4O_4)(OH)_4(H_2O)_2] \cdot 1.5\ H_2O$) strongly influences the formation and crystallization of the oxidic phase γ-Fe_2O_3 compared to the less reducing atmosphere **(4CO)** generated by gyoxylate ($[Fe_2(C_2H_2O_4)_2(OH)_2(H_2O)_2]$).

Figures 7–10 present the XRD patterns of gels B_x and E_x with formation of the single γ-Fe_2O_3 phase within the pores of the silica matrix, depending on the annealing temperature, the precursor nature and the ratio Fe_2O_3/SiO_2.

In Figures 7 and 8 the XRD patterns of the samples B_{50} and E_{50} are presented, showing the evolution of the crystalline Fe_2O_3 phases depending on the annealing temperature and the nature of the precursors. In XRD patterns in Figure 7 we can notice γ-Fe_2O_3 as the single phase, crystallized within the pores of the matrix, at 573 K. This phase is maintained even at higher temperatures: 773, 973 and 1073 K. In case of the patterns from Figure 8 corresponding to sample E_{50}, thermally treated at the same conditions, the crystallinity of γ-Fe_2O_3 at lower temperatures is weak. This can be a consequence of the less reducing atmosphere created at decomposition of the Fe(III) glyoxylate compared to Fe(III) succinate. The γ-Fe_2O_3 is well crystallized at 973 and 1073 K.

In both cases, at 1173 K and 1273 K the patterns of the samples are essentially modified indicating the formation of a new phase identified as ε-Fe_2O_3 based on JCPDS 16–653 and the recent work of Brázda et al.[19,20]

In Figure 9 the XRD patterns of the gel B_{70} annealed at different temperatures are presented. The single γ-Fe_2O_3 phase is well crystallized at 573 and 773 K. With increasing temperature, the single α-Fe_2O_3 phase crystallizes at 973 K and remains stable at 1073 and 1173 K. In case of this composition, due to the high Fe_2O_3 content, there is no efficient embedding of the particles within the pores of the silica matrix. Thus, the oxide phase γ-Fe_2O_3 is much more exposed to the transformation to α-Fe_2O_3. It is notable that in this case, the α-Fe_2O_3 is stabilized at high temperatures without transformation to other phases. For all compositions B_x, E_x where γ-Fe_2O_3 was well crystallized independent on the annealing temperature, we have calculated the size of the nanoparticles **from the (311) and (440) diffraction peaks** using the Scherrer formula,[21] and we have obtained the mean diameter of ~5 nm.

Figure 10 presents the XRD patterns of the gels B_{20}, B_{30}, B_{50} and B_{70} at 1073 K. **The patterns of the samples with 20, 30 and 50 wt% Fe_2O_3/SiO_2 reveal the well crystallized γ-Fe_2O_3 phase, but for the 50 wt% Fe_2O_3/SiO_2, the diffraction peak at 17° indicates the appearance of a weakly crystallized ε-Fe_2O_3 phase.** The XRD pattern of the sample with 70 wt% Fe_2O_3/SiO_2 presents the α-Fe_2O_3 as the single crystalline phase.

Figures 11 and 12 present the TEM images of the samples B_{30} and B_{50} annealed at 1073 K. In the sample B_{30} (30% γ-Fe_2O_3/SiO_2), the γ-Fe_2O_3 nanoparticles are spherical and homogenously dispersed within the silica matrix, with diameter of ~ 10 nm. For the sample B_{50} (50% γ-Fe_2O_3/SiO_2), the γ-Fe_2O_3 nanoparticles are more agglomerated, of spherical shape with diameters in the range 10–12 nm.

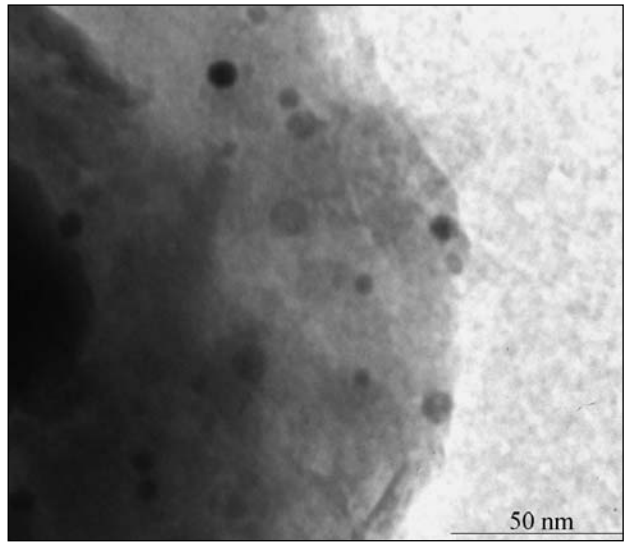

Figure 11. TEM image of the sample B_{30} annealed at 1073 K

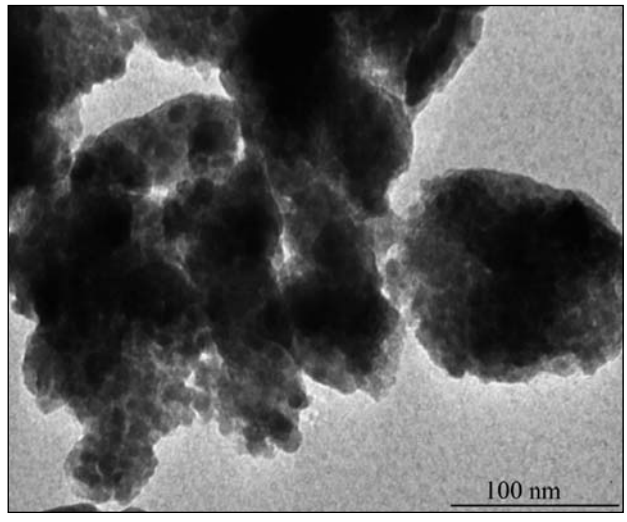

Figure 12. TEM image of the sample B_{50} annealed at 1073 K

In Figure 13 we present the magnetization curves of samples B_{50} annealed at 773 and 973 K, measured at room temperature. For both samples the coercive field is $H_c = 0$

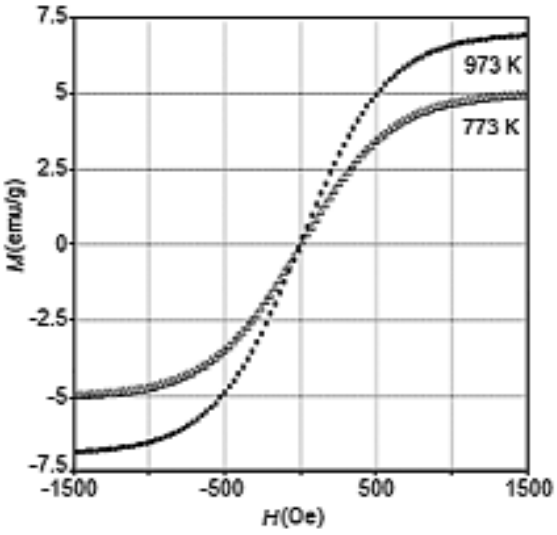

Figure 13. Magnetization curves of the sample B_{50}

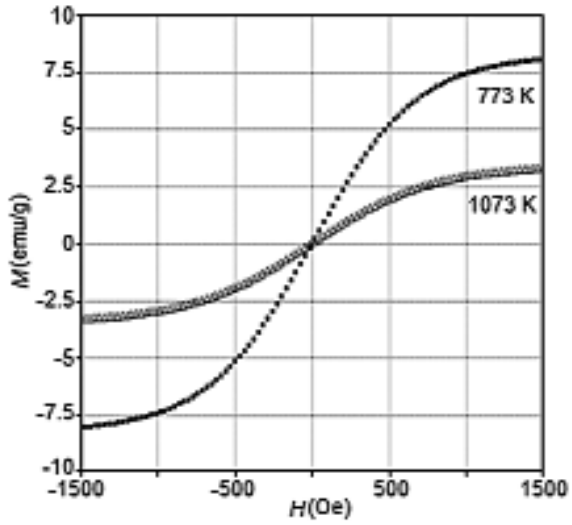

Figure 14. Magnetization curves of the sample B_{70}

leading to the superparamagnetic behavior. The value of the saturation magnetization (emu/g) increases with temperature due to the crystallinity of γ-Fe_2O_3.

A higher γ-Fe_2O_3/SiO_2 content in the sample B_{70} (Figure 14) leads to the saturation magnetization increase compared to the sample B_{50} (Figure 13) , at the same annealing temperature (773 K), H_c = 0, and the behavior is superparamagnetic.

It is notable that the sample B_{70} annealed at 1073 K exhibits a magnetic behavior although the XRD pattern (Figure 9) reveals the α-Fe_2O_3/SiO_2 **(antiferromagnetic)** as the only phase. This can be explained by the fact that γ-Fe_2O_3 is present in the matrix in a very low amount and it is of nanometric dimensions. Magnetic measurements agree with the XRD results for the samples B_{50} and B_{70}.

4. Conclusions

We report a new method to obtain the single phase γ-Fe_2O_3/SiO_2 in the temperature range 573–1073 K. The nature of the carboxylate precursors (glyoxylate, succinate) and the reducing environment created by their decomposition in the pores of the gel, influence the formation and crystallization of the γ-Fe_2O_3 nanoparticles.

For ratios ≤ 50 wt% Fe_2O_3/SiO_2, γ-Fe_2O_3 nanoparticles are formed and are stable up to 1073 K. In the cases when the samples are annealed at higher temperatures (1173 K), we observe the transformation of the γ-Fe_2O_3 to the pure oxide phase ε-Fe_2O_3. For higher ratios (70 wt%) the crystalline γ-Fe_2O_3 phase is stable up to 773 K. At higher temperatures, the γ-Fe_2O_3 transforms to the well crystallized stable α-Fe_2O_3/SiO_2.

The silica matrix remains amorphous even at high temperatures (1273 K).

The method allows obtaining the ferrimagnetic γ-Fe_2O_3/SiO_2 phase at high temperatures as well as a homogenous distribution of the nanoparticles even at high Fe_2O_3/SiO_2 ratios.

5. Aknowledgement

This work was supported by the National Project no. 71–026 NANOPART, Romanian Ministry of Education and Research.

6. References

1. S. Onodera, H. Kondo, T. Kawana, *MRS Bull.* **1996**, *21*, 35–40.
2. R. F. Ziolo, E. P. Giannelis, B. A. Weinstein, M. P. O'Horo, B. N. Ganguly, V. Mehrotra, M. W. Russel, D. R Huffman, *Science* **1992**, *257,* 219–222.
3. R. D. McMichael, R. D. Shull, L. J. Schwartzendruber, L. H. Benett, R. E. Watson, *J. Magn. Magn. Mater.* **1992**, *111*, 29–33.
4. I. J. Bruce, J. Taylor, M. Todd, M. J. Davies, E. Borioni, C. Sangregorio, T. Sen, *J. Magn. Magn. Mater.* **2004**, *284*, 145–160.
5. C. R. F. Lund, J. A. Dumesic, *J. Phys. Chem.* **1982**, *86*, 130–135.
6. R. Y. Hong, H. P. Fu, G. Q. Di, Y. Zheng, D. G. Wei, *Mat. Chem. Phys.* **2008**, *108*, 132–141.
7. N. Hüsing, U. Schubert, *Angew. Chem. Int. Ed.* **1998**, *37*, 22–45.
8. J. L. Dormann, *Mater. Sci. Eng. A* **1993**, *168*, 217–224.
9. L. I. Casas, A. Roig, E. Molins, J. M. Greneche, J. Asenjo, J. Tejada, *Appl. Phys. A* **2002**, *74*, 591–597.
10. J. M. Xue, Z. H. Zhou, J. Wang, *Mater. Chem. Phys.* **2002**, *75,* 81–85.
11. M. Birzescu, M. Cristea, M. Stefanescu, Gh. Constantin, *Ro. Pat.* 102501, **1990**.

12. C. Caizer, M. Stefanescu, J. Phys. D: Appl. Phys. **2002**, *35*, 3035–3040.
13. M. Stefanescu, O. Stefanescu, M. Stoia, C. Lazau, *J. Therm. Anal. Calorim.* **2007**, *88*, 27–32.
14. O. Stefanescu, C. Davidescu, M. Stefanescu, M. Stoia, *J. Therm. Anal. Calorim.* **2009**, *97* (1), 203–208.
15. M. Stefanescu, C. Caizer, M. Stoia, O. Stefanescu, *Acta Mater.* **2006**, *54*, 1249–256.
16. K. Nakamoto, Y. Morimoto, A. E. Martell, *J. Am. Chem. Soc.* **1961**, *83*, 4528–4532.
17. M. Stefanescu, M. Stoia, O. Stefanescu, *J. Sol-Gel Sci. Technol.* **2007**, *41*, 71–78.
18. D. Knetsch, W. L. Groeneveld, *Inorg. Chim. Acta* **1973**, *7*, 81–87.
19. R. Schrader, G. Buttner, Z. Anorg. Allgem. Chem. **1963,** *320,* 220–234.
20. P. Brázda, D. Nižòansky, J-L. Rehspringer, J. P. Vejpravova, *J. Sol-Gel Sci. Technol.* **2009**, *51*, 78–83.
21. R. Jenkins, R. L. Snyder, *Introduction to X-ray Powder Diffractometry*, John Wiley & Sons Inc., New York, **1996**, pp. 89–91.

Povzetek

V delu opisujemo sintezo in temperaturno obstojnost nanodelcev γ-Fe_2O_3 v gelih SiO_2. Slednja je odvisna od vrste Fe(III) karboksilatnega prekurzorja, temperature segrevanja in koncentracije Fe^{3+}. Priprava prekurzorjev v porah gela temelji na redoks reakciji med $Fe(NO_3)_3$ in dioloma etilenglikolom (EG) in 1,4-butandiolom (1,4 BG). Pripravili smo gele z različnimi razmerji Fe_2O_3/SiO_2 (20, 30, 50, 70 utežnih % Fe_2O_3) in jih segrevali pri temperaturah med 573 in 1273 K.

Na nastanek in stabilnost enofaznega γ-Fe_2O_3 v porah gela močno vpliva redukcijska atmosfera, ki se vzpostavi med termičnim razpadom Fe(III) karboksilatov. Rentgenska fazna analiza je potrdila izrazitejšo kristalizacijo γ-Fe_2O_3, ko je bil uporabljen 1,4 BG. Magnetne meritve so potrdile kristalinično fazo γ-Fe_2O_3 v matrici silicijevega oksida.